

Article

Measurement of Temperature and H₂O Concentration in Premixed CH₄/Air Flame Using Two Partially Overlapped H₂O Absorption Signals in the Near Infrared Region

Sunghyun So ^{1,2}, Nakwon Jeong ^{1,2}, Aran Song ^{1,2}, Jungho Hwang ², Daehae Kim ^{1,*} and Changyeop Lee ^{1,*}

¹ Industrial Environment Green Deal Agency, Korea Institute of Industrial Technology, Cheonan 31056, Korea; shso@kitech.re.kr (S.S.); skrdnjs0456@kitech.re.kr (N.J.); arnsong88@kitech.re.kr (A.S.)

² Department of Mechanical Engineering, Yonsei University, Seoul 03722, Korea; hwangjh@yonsei.ac.kr

* Correspondence: kimdh@kitech.re.kr (D.K.); cylee@kitech.re.kr (C.L.)

Abstract: It is important to monitor the temperature and H₂O concentration in a large combustion environment in order to improve combustion (and thermal) efficiency and reduce harmful combustion emissions. However, it is difficult to simultaneously measure both internal temperature and gas concentration in a large combustion system because of the harsh environment with rapid flow. In regard, tunable diode laser absorption spectroscopy, which has the advantages of non-intrusive, high-speed response, and in situ measurement, is highly attractive for measuring the concentration of a specific gas species in the combustion environment. In this study, two partially overlapped H₂O absorption signals were used in the tunable diode laser absorption spectroscopy (TDLAS) to measure the temperature and H₂O concentration in a premixed CH₄/air flame due to the wide selection of wavelengths with high temperature sensitivity and advantages where high frequency modulation can be applied. The wavelength regions of the two partially overlapped H₂O absorptions were 1.3492 and 1.34927 μm. The measured signals separated the multi-peak Voigt fitting. As a result, the temperature measured by TDLAS based on multi-peak Voigt fitting in the premixed CH₄/air flame was the highest at 1385.80 K for an equivalence ratio of 1.00. It also showed a similarity to those tendencies to the temperature measured by the corrected R-type T/C. In addition, the H₂O concentrations measured by TDLAS based on the total integrated absorbance area for various equivalent ratios were consistent with those calculated by the chemical equilibrium simulation. Additionally, the H₂O concentration measured at an equivalence ratio of 1.15 was the highest at 18.92%.



Citation: So, S.; Jeong, N.; Song, A.; Hwang, J.; Kim, D.; Lee, C. Measurement of Temperature and H₂O Concentration in Premixed CH₄/Air Flame Using Two Partially Overlapped H₂O Absorption Signals in the Near Infrared Region. *Appl. Sci.* **2021**, *11*, 3701. <https://doi.org/10.3390/app11083701>

Academic Editor: Steven Wagner

Received: 28 March 2021

Accepted: 19 April 2021

Published: 20 April 2021

Publisher's Note: MDPI stays neutral with regard to jurisdictional claims in published maps and institutional affiliations.



Copyright: © 2021 by the authors. Licensee MDPI, Basel, Switzerland. This article is an open access article distributed under the terms and conditions of the Creative Commons Attribution (CC BY) license (<https://creativecommons.org/licenses/by/4.0/>).

Keywords: tunable diode laser absorption spectroscopy; temperature; concentration; partially overlapped absorption; premixed flame

1. Introduction

The energy sources used worldwide are typically hydrocarbon fuels, renewable energy, and nuclear fission. Among them, hydrocarbon fuels are expected to be used at a rate of 50% or more by 2040 [1]. Generally, hydrocarbon fuels produce energy through a combustion system, and the combustion emissions cause air pollution. Coal power plants are large-scale combustion systems that convert energy using hydrocarbon fuels. Currently, coal power plants face difficulties in reducing air pollutants while maintaining high-efficiency energy production. Therefore, it is important to monitor the temperature and H₂O concentration in a large combustion environment to improve the combustion (and thermal) efficiency and reduce harmful combustion emissions. Temperature is a fundamental parameter of the combustion system and an important factor in determining the overall thermal efficiency. However, it affects the production of pollutants, such as nitrogen oxides, in association with the formation of localized high temperatures in the combustion field. In addition, the H₂O concentration in the combustion environment is an indicator of the overall combustion efficiency as a primary product of the combustion reaction. However, it is difficult to

simultaneously measure both the internal temperature and gas concentration in a large combustion system because of the severe environment. In general, a thermocouple (T/C) and dew point sensor are used for measuring the temperature and H₂O concentration. However, it is difficult to predict the overall reaction inside the combustion environment using the results provided due to physical probing and sampling method at fixed points. In addition, these methods have short durability due to the severe environment and high temperatures, and cause flow disturbances in the combustion field. To overcome these limitations, researchers have developed a non-intrusive method using tunable diode laser absorption spectroscopy (TDLAS), which is an optical measurement method that utilizes absorption with a narrow linewidth. It is also highly selective, durable, and fast responsive, and is widely applied in various combustion environments such as IC engine, biomass, scramjet, and coal gasifier [2–7]. From the theory of TDLAS, a single absorption signal and the ratio of two absorption signals are used to measure the gas concentration and flow field temperature in combustion environments [3,8]. In this case, as H₂O molecules are present in a considerable proportion in the combustion environment, the use of their two absorption signals is advantageous to derive the temperature.

Temperature measurements using TDLAS have been previously performed in various combustion environments. Webber et al. (2000) obtained the temperature from two H₂O absorption signals in each scan range by using two lasers (1.343 and 1.392 μm) and wavelength division multiplexing to measure the temperature and concentration in the C₂H₄/Air flame [9]. Torek et al. (2002) measured the temperature and H₂O concentration of silane/hydrogen/oxygen/argon flames using the H₂O absorption wavelength region of 1.392–1.394 μm [10]. Here, Torek et al. used two H₂O absorption signals separated from each other within the single scan range of one laser. Unlike previous studies in the wavelength range of 1.300–1.400 μm, Goldenstein et al. (2013) measured the internal temperature under various pressures and temperature conditions in a three-zone electric furnace using the new H₂O absorption wavelength regions of 2.474 and 2.482 μm. Here, the temperature was derived from two H₂O absorption signals in each scan range by using two lasers with wavelengths of 2.474 and 2.482 μm [11]. In addition, Wu et al. (2014) measured the temperature using the CO₂ absorption wavelength region of 4.174 to 4.184 μm in the mid-infrared region, unlike the above mentioned study, in which the temperature was measured using H₂O absorption wavelengths in the near-infrared region [12]. Ma et al. (2017) used two lasers at H₂O absorption wavelength regions of 2.482 and 1.343 μm to measure the H₂O concentrations and temperatures in the CH₄/air flame [13].

Recently, applied temperature measurement methods based on the two-line thermometry method have been developed [14,15]. This applied temperature measurement method typically consists of a temperature binning and tomography method for analyzing non-uniform temperature and concentration fields, and an intensity-modulation spectroscopy method for increasing the sensitivity of temperature measurement in high temperature/high pressure environments. These methods also used each absorption from two lasers to fundamentally increase the temperature measurement sensitivity.

Temperature measurement by TDLAS was started with the two-line thermometry method using two absorption signals, as described above. Previous studies have measured the temperature using two absorption signals separated from each other within a single scan range of one laser. In addition, the temperature was also obtained from two absorption signals in each scan range using two lasers. Because the two absorption areas derived from the two absorption signals change sensitively according to the temperature change, it is difficult to accurately analyze the two sensitive absorption areas when the absorption signals partially or completely overlap; this results in an error in the temperature readings. For these reasons, most studies have used two absorption signals that were separated from each other. This corresponds to the “appropriate spectral separation” in the line selection method for measuring the temperature, summarized by Zhou et al. [16]. However, the two H₂O absorption signals separated from each other within a single scan range of one laser are limited to the wavelength region of 1.300–1.400 μm, in which the H₂O

absorption is most abundant. Temperature measurements systems using multiple lasers are complex and have increased costs. A situation in which the two H₂O absorption signals overlap within a single scan range in the near-infrared region of 1.300–1.400 μm can be advantageous if the temperature and concentration can be measured simultaneously. First, there are several high-sensitivity absorption lines that were not previously selected because of the overlapping of H₂O absorption signals in the near-infrared region. Second, the TDLAS method scans an absorption signal with the corresponding wavelength by modulating a waveform with a constant period and amplitude. Thus, the wavelength scan range decreases as the frequency modulation (constant period) increases. However, high-frequency modulation is essential for measurement in fast flow fields, such as large-scale combustion systems [17]. Therefore, it is easy for the partially overlapped H₂O absorption signals to be contained in a narrow wavelength region in the single scan range of a high-frequency modulation. However, despite these advantages, studies on the measurement of temperature and H₂O concentration using two partially overlapped H₂O absorption signals under general normal pressure conditions are insufficient. In the present study, the wavelength regions of the two partially overlapped H₂O absorptions were selected as 1.34923 and 1.34927 μm in a single scan range. First, the set temperatures (1073.15–1573.15 K) in the electric furnace were measured using two partially overlapped H₂O absorption signals. Second, the temperature and H₂O concentration in the premixed CH₄/air flame were measured using two selected H₂O absorption wavelengths. In this method, the temperature was measured after separating the two partially overlapped H₂O absorption signals at the selected wavelength by using the multi-peak Voigt fitting and reconstruction method using half absorbance. The H₂O concentration was derived from the total integrated area of two partially overlapped H₂O absorption signals.

2. Theory

2.1. Recovery of Curve Fitting for Partially Overlapped Absorption Signal

2.1.1. Reconstruction Method Using Half Absorbance

The energy of the optical transition is the same as the energy difference between the upper and lower states, and Heisenberg's uncertainty principle can be associated with the lifetime from the uncertainty of these energy levels [18]. The uncertainty of energy level i can be expressed by Equation (1):

$$\Delta E_i \geq \frac{h}{2\pi\tau_i} \quad (1)$$

where τ_i is the lifetime of the energy level i , which can be expressed as the total energy uncertainty ΔE_i of the transition by combining the lifetimes τ' and τ'' of the upper and lower states, respectively. Therefore, the probability that the transition is measured can be expressed as a nonzero-energy range. The range can be summarized as the full width at half maximum (FWHM) of the line width given (in frequency units), as in Equation (2), when Planck's law $\Delta E = h\Delta\nu$ is substituted into Equation (1) [19]:

$$\Delta\nu = \frac{1}{2\pi} \left(\frac{1}{\tau'} + \frac{1}{\tau''} \right) \quad (2)$$

All lineshapes have the shape of a probability density function based on Heisenberg's uncertainty principle. Therefore, spectral lines have symmetry for a single transition. It becomes possible to reconstruct the two partially overlapped H₂O absorptions through this symmetry.

2.1.2. Multi-Peak Voigt Fitting

The absorbance α_ν for multiple transitions can be further expanded, as shown in Equation (3) [20]:

$$\alpha_\nu = \sum_{i=1}^M \alpha_i \phi_V(\nu; \nu_{0,i}, \gamma_i) \quad (3)$$

$\phi_V(\nu; \nu_{0,i}, \gamma_i)$, which is generally explained by the Voigt function, can be represented by an individual absorption peak with a wavelength ν . Here, α_i is the peak height, $\nu_{0,i}$ is the peak position, and γ_i is the half-width at half maximum (HWHM). In addition, M and i are the number of peaks and the serial number of each peak, respectively. Therefore, the Voigt function can be expressed by Equation (4):

$$\phi_V(\nu; \nu_{0,i}, \gamma_i) = A \frac{y}{\pi} \int_{-\infty}^{+\infty} \frac{\exp(-t^2)}{y^2 + (x-t)^2} dt = A \cdot \text{Re}[W(x, y)] \quad (4)$$

For Equation (4), $W(x, y) = \frac{i}{\pi} \int_{-\infty}^{+\infty} \frac{\exp(-t^2)}{x+iy-t} dt$ can be obtained. The Voigt function parameter in Equation (4) is composed of $A = \frac{\sqrt{\ln 2}}{\gamma_D \sqrt{\pi}}$, $x = \sqrt{\ln 2} \frac{\nu - \nu_0}{\gamma_D}$, and $y = \sqrt{\ln 2} \frac{\gamma_L}{\gamma_D}$. Here, γ_D and γ_L are the Doppler HWHM and Lorentzian's HWHM, respectively. As expressed by Equation (5), γ_D is a function of the temperature T and molecular weight M_{mole} :

$$\gamma_D = \frac{\nu_0}{c} \sqrt{\frac{2k \ln 2}{M_{mole}}} = 3.5812 \times 10^{-7} \nu_0 \sqrt{\frac{T}{M_{mole}}} \quad (5)$$

As expressed in Equation (6), γ_L can be expressed as self-collision HWHM, foreign gas collision HWHM, partial pressure of absorbed gas species, and total pressure by subdividing Lorentzian's HWHM:

$$\gamma_L = \gamma_{self} P_{self} \left(\frac{T_0}{T} \right)^n + \gamma_{self} (P - P_{self}) \left(\frac{T_0}{T} \right)^n \quad (6)$$

where n is the corresponding coefficient of temperature dependence. The ratio of y in Equation (4) is determined from the proportional relationship between the Lorentzian and Gaussian features of the lineshape. If y is lower than 1, the Voigt function can be represented as Gaussian, and if y is higher than 1, it can be represented as a Lorentzian. That is, the parameter of each individual peak is determined at the same time by minimizing the square variance between the measured absorbance and the model calculation. As a result, an appropriate curve fitting method should be applied to accurately determine the two partially overlapped H₂O absorption signals based on the above equations [21].

3. Line Selection

The proposal of this study is to measure the temperature using two partially overlapped H₂O absorption signals within a single scan range. Line selection methods summarized in the study by Zhuo et al. were applied to measure the optimum temperature [16]. This method can be divided into five criteria, which can be expressed as follows.

- (1) The two selected absorption lines should have sufficient absorption signals in the temperature range;
- (2) The two absorption lines are within a single laser scan range and do not overlap with each other in the atmosphere;
- (3) The R of the integrated absorbance area should be single-valued with temperature, and the line strengths of the two absorption lines ($R = 0.2\text{--}5.0$) should be similar;
- (4) The two absorption lines have sufficiently different lower-state energy E'' to yield an absorption ratio that is sensitive to the probed temperature;
- (5) There should be no interference from other gas molecules near the two absorption signals.

As mentioned above, two suitable partially overlapped H₂O absorption lines (1.34923 and 1.34927 μm) were selected meeting the criteria established, except the second one.

For the first criterion, Zhuo et al. described the peak absorption of transition, which includes the gas mole fraction, linestrength, pressure, and optical path length in the measurement environment based on optically thick conditions. The range for the peak absorption of transition was set to be higher than 0.001 and lower than 0.800. To satisfy this range, the H₂O concentration (range: approximately 10–20%) produced after the premixed CH₄/air flame reaction was predicted using a chemical equilibrium solver (Chemkin). The linestrength magnitude (cm/molecule, 10^{−22}) that did not violate the range for peak absorption of transition in the corresponding H₂O concentrations was also confirmed [16]. In addition, the optical path length that satisfies the range for the peak absorption of transition was considered. Figure 1 shows a graph of the linestrengths of the two H₂O absorption lines at 296, 1073, 1473.15, and 1773.15 K using the HITRAN2012 database and compared with the linestrengths of other combustion products [22]. As shown in Figure 1, the linestrengths of the two selected absorption lines between 1073.15 and 1773.15 K had a similar magnitude of 10^{−22}. It was also confirmed that there was no interference from other combustion products (fifth criterion).

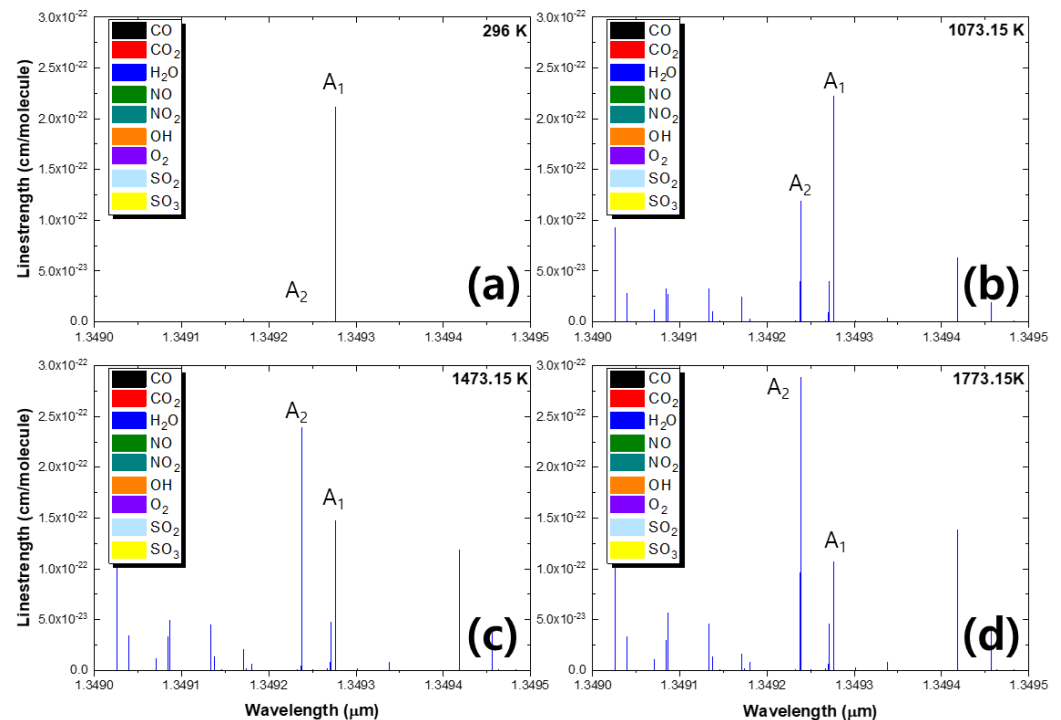


Figure 1. (a) Linestrengths of H₂O and combustion products within 1.3490–1.3495 μm at 296 K, (b) 1073.15 K, (c) 1473.15 K, and (d) 1773.15 K from the HITRAN2012 database.

Figure 2 is a graph presenting the analysis of the third and fourth criteria. Figure 2a shows the sensitivity of the linestrength ratio for the difference in lower-state energy as a function of temperature. The lower-state energy between the two absorption wavelengths for the fourth criterion must have a sufficient difference as it is related to the sensitivity of the probed temperature. As can be seen from the relative sensitivity equation [18], the large difference in lower-state energy improves the sensitivity to temperature measurement. Most previous studies have found that the difference in lower-state energy at optimal absorption line pair is between 1000 and 2000 cm^{−1}. At 1.34923 and 1.34927 μm selected for our study, the lower-state energies were $E_1 = 3655.4833 \text{ cm}^{-1}$ and $E_2 = 602.7735 \text{ cm}^{-1}$, respectively, with a difference of 3052.709 cm^{−1}. This large difference in lower-state energy can have a high sensitivity for temperature measurement, but it can also have drawbacks depending on the temperature, optical path-length, and concentration in the measurement environment [23]. As shown in temperature equation [24], the temperature is determined by the ratio of the integrated absorbance area. The relationship between the integrated

absorbance and the lower-state energy can generally be expressed by two effects. When one of the two absorption signals has a high lower-state energy, it has a low absorbance. In contrast, when the other absorbed signal has a small lower-state energy, it has a high absorbance. In other words, if the integrated absorbance is very small or large, it will cause an error in the analysis of the results. Thus, similar signal to noise ratio (SNR) is desired for both absorption signals [25]. In this study, the linestrengths of the two selected H₂O absorptions had a similar magnitude (10^{-22}) as the analysis result shown in Figure 2b increased to 900 K or more. They were expected to be suitable for absorbance analysis based on the predicted H₂O concentration and optical path length in the measurement environment. In addition, the third criterion was satisfied for a linestrength ratio of $R = 0.2\text{--}5.0$ for optimum temperature measurement. Table 1 shows the conditions of the two H₂O absorption lines selected to measure the temperature using two partially overlapped H₂O absorption signals.

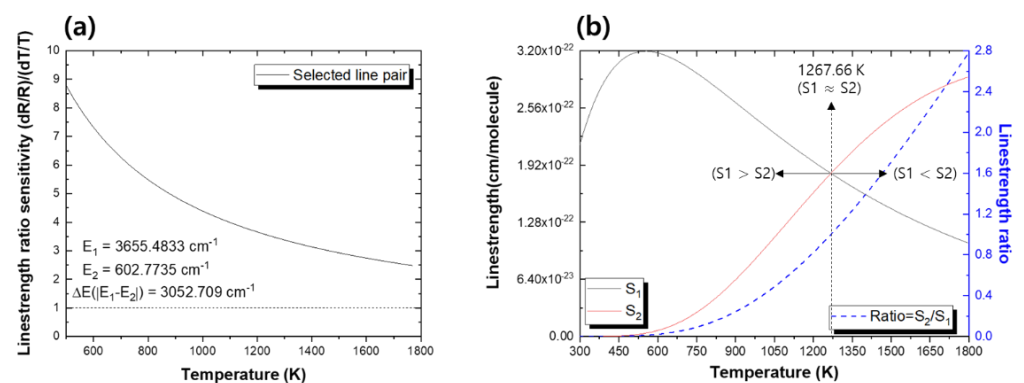


Figure 2. (a) Calculated temperature sensitivity of the linestrength ratio at the temperature range 550–1800 K, and (b) calculated linestrength ratios for the two selected absorption lines at 300–1800 K.

Table 1. Two selected H₂O absorption lines for measuring the temperature and concentration from the HITRAN database.

$\lambda, (\mu\text{m})$	$\nu, (\text{cm}^{-1})$	$S(T)$ at 1073.15 K, (cm/molecule)	$E'' ,(\text{cm}^{-1})$	$\Delta E'' ,(\text{cm}^{-1})$	Line Spacing, (cm^{-1})
1.34923	7411.589	1.188×10^{-22}	3655.4833	3052.709	0.2126
1.34927	7411.376	2.227×10^{-22}	602.7735		

4. Experimental Setup and Condition

4.1. Preliminary Experimental Setup

The experimental process in this study can be divided into two steps. The first step was to confirm the accuracy of the measured temperature using two partially overlapped H₂O absorption signals. Here, the temperature set in the electric furnace by the T/C gauge was compared to the temperature measured by TDLAS. The temperatures (1073.15, 1173.15, 1273.15, 1373.15, 1473.15, and 1573.15 K) including the predicted flame temperature range, were set in the electric furnace. Figure 3 shows a schematic diagram of an overall preliminary experiment for measuring the temperature set in an electric furnace.

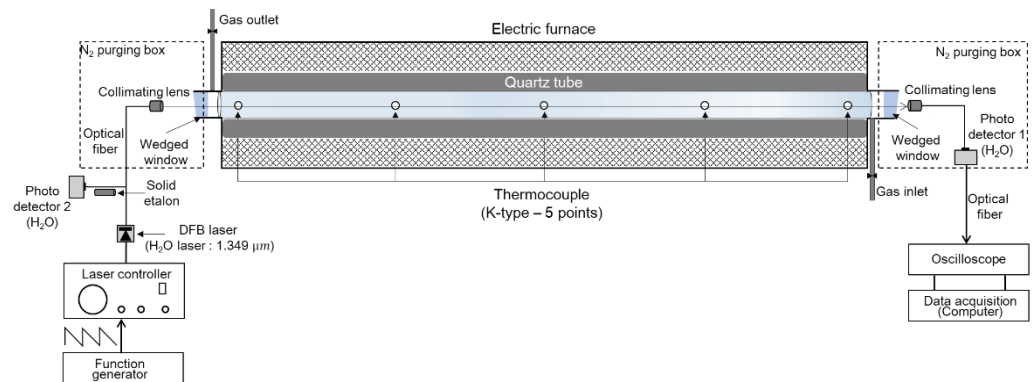


Figure 3. Schematic diagram of the measurement system applied to an electric furnace.

As shown in the schematic diagram in Figure 3, the inside of the electric furnace was composed of ceramic board insulation to maintain a steady state (for internal temperature), and a quartz tube (170 cm) was inserted in the center of the electric furnace. In addition, calcium fluoride (CaF_2) wedged windows were installed at both ends of the electric furnace because the reflected light generated between the light source and the window causes signal distortion (etalon noise). The temperature was set as the measured value from the R-type T/C installed in the insulation at the center of the electric furnace. Next, in the case of a laser system, the laser was largely divided into a transmitter and a receiver. For the transmitter part, the laser of the irradiated light source was a distributed feedback laser (butterfly 14 pin, NTT), which contained wavelengths of 1.34923 and 1.34927 μm within a single scan range. A laser controller (ILX Lightwave, LDC-3908) was used to apply a constant current and temperature to the laser to emit the light source of the selected H_2O absorption wavelength. Here, the current and temperature of the laser controller were determined using a wavemeter (HighFinesse laser and electronic system, WS-6) to accurately confirm the selected wavelength region. In addition, a waveform with a constant period and amplitude was applied to the laser controller using a function generator (Tektronix, AFG320) for wavelength tuning and signal analysis of the absorption signal. The receiver part was composed of a photodetector (Thorlabs, PDA20CS-EC) to detect light sources and a data acquisition (DAQ) system for data acquisition. Then, the light source transmitted through the inside of the electric furnace was focused on the photodetector on the receiver. Here, photodetector 2 was used to receive the initial intensity also, light source was detected at the photodetector 2 through the solid etalon with a free spectral range (FSR, 2.00 GHz) to convert the time domain of the light absorption signal into the wavelength domain. Additionally, photodetector 1 was used to analyze the transmitted intensity, including the H_2O absorption signal. The signals acquired by the DAQ system (500 kS/s) were analyzed using MATLAB.

4.2. Combustion Experimental Setup

After the preliminary experiment, the combustion experiment was performed with a metal fiber burner to analyze the characteristics of temperature and H_2O concentration generated from the premixed CH_4 /air flame. Figure 4 shows the combustion setup part of the metal fiber burner for generating the premixed CH_4 /air flame and the laser setup. The heat load of the metal fiber applied to the experiment was approximately 9000 kcal/h with an equivalence ratio of 1.00. The fuel was supplied as CH_4 gas to the center below the metal fiber burner. After general compressed air was converted to dry air via a drying system, the oxidizer was supplied to the sides of the metal fiber burner. This dry air was mixed with CH_4 gas at the center of the metal fiber burner. The premixed CH_4 gas and dry air were formed into a flame from the porous surface of the metal fiber burner. The flow rates of the fuel and oxidizer for controlling the equivalence ratio (Φ) were controlled by a mass flow controller (MFC), and N_2 gas was injected on the side of the burner to eliminate the inflow of external air into the flame.

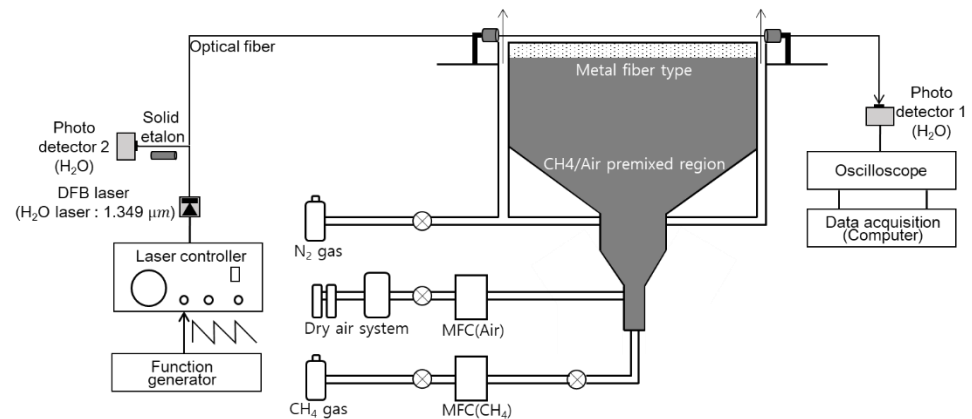


Figure 4. Schematic diagram of the measurement system applied to a metal fiber burner.

The laser setup part based on TDLAS was applied with the same setup as in the preliminary experiment. The light source was transmitted directly into the premixed CH_4/air flame to measure the temperature and H_2O concentration. A gold mirror with high reflectance was used to ensure a high SNR of the absorption signal because the integrated absorbance increased as the optical path length increased (94 cm). The light source was also transmitted to a height of 5 mm above the surface of the metal fiber burner.

Table 2 shows the conditions of the combustion experiment. The fuel was fixed at 8.46 L/min for a heat load of 9000 kcal/h, and the equivalence ratio was determined by adjusting the oxidizer. The equivalence ratio was set at 0.15 intervals from the fuel lean condition of 0.70 to the fuel-rich condition of 1.30.

Table 2. Operating conditions for the combustion experiment of premixed CH_4/air flame.

Equivalence Ratio (Φ)	Fuel (L/min)	Air (L/min)
0.70	8.46	252.57
0.85		208.68
1.00		176.44
1.15		154.58
1.30		137.03

5. Results and Discussion

5.1. Results of Preliminary Experiment

Figure 5 shows the two partially overlapped H_2O absorption signals measured at the center temperatures of 1073.15, 1273.15, and 1573.15 K in the electric furnace in the preliminary experiment.

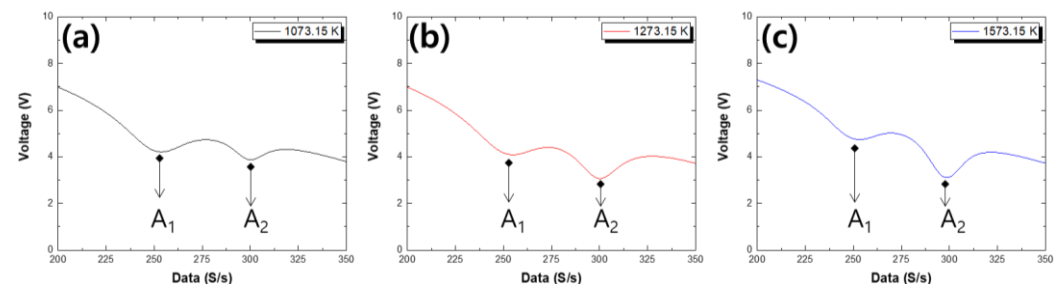


Figure 5. (a) Two partially overlapped H_2O absorption signals measured at 1073.15 K, (b) 1273.15 K, and (c) 1573.15 K in the electric furnace.

As shown in Figure 2b, the linestrengths of the two partially overlapped H_2O absorption wavelengths with increasing temperature were compared. It was found that the

magnitude of the two partially overlapped H₂O absorption signals measured according to the temperature in the electric furnace corresponded to the tendency of the ratio of the linestrength analyzed in Figure 2b. Specifically, in the linestrength ratio in Figure 2b, S1 was larger than S2 below 1275.15 K. In contrast, it can be seen that S1 and S2 were the same at 1267.66 K. It was confirmed that S1 tended to be smaller than S2 above 1273.15 K. As shown in Figure 5a, the two partially overlapped H₂O absorption signals measured at 1073.15 K showed that A1 was larger than A2, such as the ratio of the line strength in Figure 2b. Figure 5b shows that the absorption signals of A1 and A2 were almost the same at 1273.15 K. Finally, it was found that the absorption signal at 1573.15 K was larger in A2 than in A1. Thus, it was confirmed once again that the tendency of the two absorption signals and the line strength ratio analyzed in Figure 2b were the same. Figure 6 shows the result of internal temperatures measured by the T/C of the electric furnace set at 1473.15 K. TDLAS based on line of sight is a technology that provides the line-average information of a measurement target. Therefore, the temperature value measured by TDLAS in the electric furnace was compared with the temperature value measured by the T/C based on the internal length interval measurement.

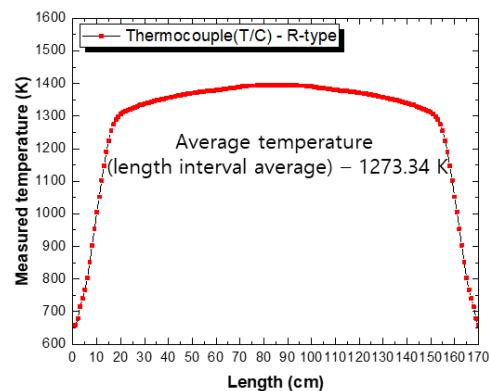


Figure 6. Measured temperature profile using thermocouple at 1473.15 K in the electric furnace.

As the measurement range of temperature is different depending on the T/C type, K-type T/C was used for temperatures from 1073.15 and 1173.15 K, and R-type T/C was used for temperatures from 1273.15 to 1573.15 K. In particular, the temperatures were measured at 1-cm intervals in an electric furnace with a length of 170 cm. As shown in Figure 6, the average temperature of the internal length intervals using a T/C at a center temperature of 1473 K was measured at 1273.34 K. The average temperature of the internal length interval was lower than the set center temperature of the electric furnace because the mounts for fastening the CaF₂ windows on both sides of the electric furnace were far from the heating element. In addition, it was a region where heat exchange with the atmosphere occurred, and heat was not preserved at both ends of the electric furnace. As a result, the comparison between the average temperature of the internal length interval measured by the T/C and the set center temperature in the electric furnace was derived, as shown in Table 3.

Table 3. Comparison of set temperature in electric furnace and temperature measured by T/C.

Set Temperature (K)	1073.15	1173.15	1273.15	1373.15	1473.15	1573.15
Measured temperature (K)	797.30	924.08	1069.39	1165.48	1273.34	1360.28

Figure 7 shows a comparison of the reconstruction method using half absorbance and the multi-peak Voigt fitting method proposed to analyze the two partially overlapped H₂O absorption signals. From Equations (1) and (2), the reconstruction method using half absorbance focused on the spectral lineshape symmetry of lifetime broadening, which

is the principle of Heisenberg's uncertainty. As shown in Figure 7a, because they have a symmetrical normal distribution based on the peak of the absorption signal, A1 and A2 can be reconstructed using each half absorbance except for the center of the two partially overlapped H₂O absorptions. Half absorbances that are bidirectionally symmetric with respect to the center absorption line of A1 and A2 were generated, and then Voigt fitting was applied. Figure 7b shows a graph that analyzes signals from a mathematical model (curve fitting method) to which individual Voigt fittings were applied using the multi-transitions theory of Equations (3) and (4).

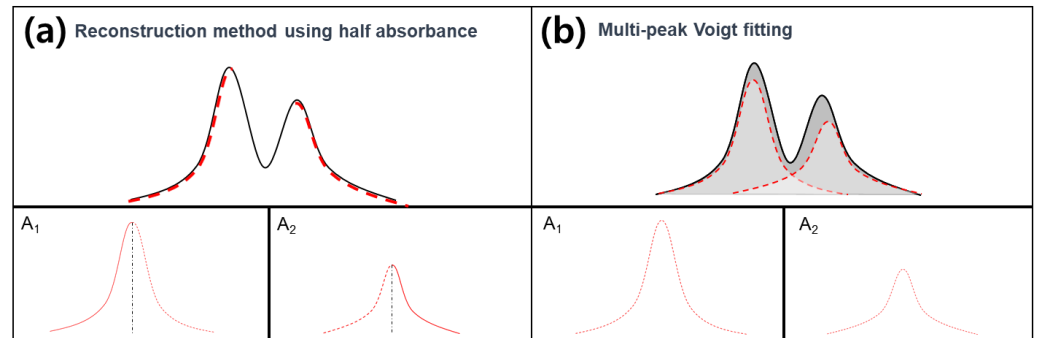


Figure 7. Comparison of reconstruction method using half absorbance and multi-peak Voigt fitting method presented for analysis of the two partially overlapped H₂O absorption signal.

As shown in Figure 7b, the peaks of absorbance areas A1 and A2 analyzed by multi-peak Voigt fitting were lower than the peak of the total absorbance area, unlike what occurred for the reconstruction method using half absorbance shown in Figure 7a. The center area of the two partially overlapped H₂O absorption signals was expected to cause the peak increase to be higher than the peak of the existing individual absorption signal. In summary, analysis methods were presented to clearly identify the characteristics of the two partially overlapped H₂O absorption signals according to the temperature. Therefore, the two partially overlapped H₂O absorption signals were analyzed by the reconstruction method using the half-absorbance and multi-peak Voigt fitting methods presented in this study [18–21].

Figure 8 shows the comparison of the temperature derived from the methods of analyzing the two partially overlapped H₂O absorption signals and the temperature measured by the T/C to precisely measure the temperature set in the electric furnace. In Figure 8a, the two partially overlapped H₂O absorption signals were separated into A1 and A2 after applying the multi-peak Voigt fitting method at 1073.15 K of the electric furnace. Because the linestrength ratio of the two partially overlapped H₂O absorption signals selected in this study changed sensitively depending on the temperature, the two absorption signals were accurately analyzed for changes in the sensitive absorption signals A1 and A2 in the set temperature range. In particular, from Figure 2b, when the linestrength was smaller or greater than 1267.66 K, at which S1 and S2 were equal, the absorbance areas A1 and A2 significantly increased or decreased, respectively. At the set center temperature in the electric furnace, Figure 8b shows a comparison of the temperature measured by TDLAS using the methods shown in Figure 7 and the average temperature of the internal length interval measured by the T/C. The temperature was derived by applying the integrated absorbance of the partially overlapped H₂O absorption signal separated by the reconstruction method using half absorbance and the multi-peak Voigt fitting method to temperature equation [24]. It was determined that the temperature value measured by TDLAS based on the methods of Figure 7 corresponded to the tendency of the average temperature value of the internal length interval measured by the T/C.

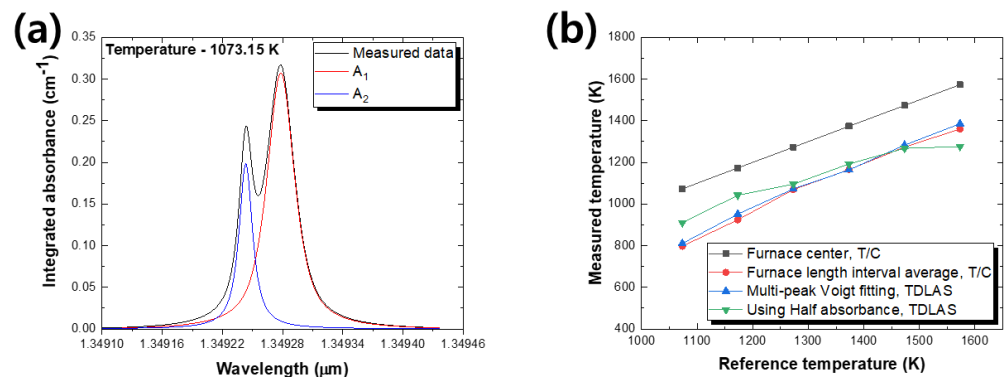


Figure 8. (a) Multi-peak Voigt fitting for measured data at 1073.15 K, and (b) comparison of the experimentally obtained temperature using TDLAS with measured temperature using T/C in the electric furnace.

In contrast, the temperature measured by TDLAS based on the methods shown in Figure 7 did not significantly decrease compared to the center temperature of the electric furnace because it was an internal line-average measurement. However, as can be seen from Figure 8b, when comparing the temperature results measured by the methods of Figure 7, the temperature measured by the reconstruction method using half absorbance was considerably higher than the temperature measured by the multi-peak Voigt fitting method at the center temperature of the electric furnace at 1073.15 and 1173.15 K. Thus, it was derived that the temperature measured from the reconstruction method using half absorbance tended to be lower than the temperature measured by the multi-peak Voigt fitting method as the temperature increased to 1573.15 K. As shown in Figure 2b, it was confirmed that the ratio of the two partially overlapped H₂O linestrengths was significantly different when the temperature decreased and increased at 1267.66 K. The reconstruction method using half absorbance did not sensitively consider the increased area due to the overlapped center area of the two partially overlapped H₂O absorption signals when the absorbance area A₁ was considerably larger than A₂ (Figure 8a), such as the absorption signals measured at 1073.15 K. The absorbance area A₂ increased excessively with the amount of absorbance area A₁ overlapped with the original absorbance area A₂. It was expected an error in temperature measurement caused by the reconstruction method using half absorbance, as a result of analyzing the increased absorbance area A₂ due to the absorbance area A₁ instead of the original A₂ absorbance area. As shown in Figure 8a, the multi-peak Voigt fitting method showed a large difference, unlike the reconstruction method using half absorbance, because it considered the increased area at the center of the two partially overlapped H₂O absorption signals. However, as can be seen from the analysis results of Figure 8b, it was considered that the center area of the two partially overlapped H₂O absorption was not significantly affected because the two H₂O absorption signals analyzed by the reconstruction method using half absorbance had similar linestrength in the temperature range of 1250–1350 K.

Figure 9 is a graph of the absorption signals at 1073.15 and 1473.15 K analyzed by the reconstruction method using half absorbance. As can be seen from Figure 9a, when A₁ was larger than A₂, the large absorption area A₁ affected the increase of the absorption area A₂, which caused an error. However, as shown in Figure 9b, when the absorbance areas A₁ and A₂ were similar, they increased in the same proportion. Therefore, the difference between the temperature measured by the two methods analyzed within 1250–1350 K showed a similar tendency. As a result, the two partially overlapped H₂O absorption signals throughout the preliminary experiment were more accurately analyzed for areas A₁ and A₂ derived from the multi-peak Voigt fitting method. It was confirmed that the temperature measured by multi-peak Voigt fitting showed a linear tendency similar to the center temperature of the electric furnace and had higher temperature measurement sensitivity.

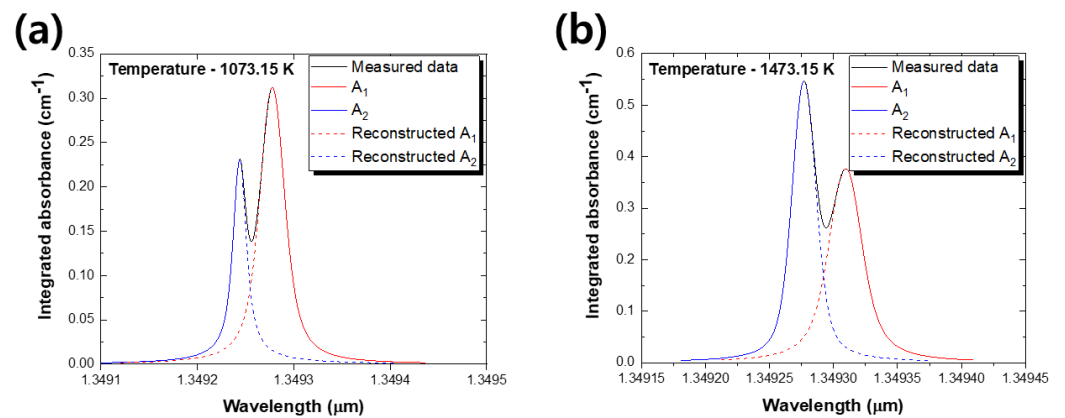


Figure 9. Reconstruction method using half absorbance for measured data at (a) 1073.15 K and (b) 1473.15 K.

5.2. Results of Combustion Experiment

The temperature and H₂O concentration in the premixed CH₄/air flame were derived from the two partially overlapped H₂O absorption signals with high sensitivity, as confirmed by the multi-peak Voigt fitting method using an electric furnace (Figure 10). Figure 10a shows the two partially overlapped H₂O absorption signals at an equivalence ratio of 1.00, for the premixed CH₄/air flame. Similar as in the temperature analysis of the preliminary experiment, the integrated absorbance areas A₁ and A₂ were separated using a multi-peak Voigt fitting, and the flame temperature was derived by applying the separated integrated absorbance areas A₁ and A₂ to temperature equation [24]. Thereafter, the derived flame temperature was used to calculate the linestrength equation [26], and the obtained linestrength was used to calculate the H₂O concentration using concentration equation [27]. Figure 10b shows the two partially overlapped H₂O absorption signals at an equivalence ratio of 1.00, as shown in Figure 10a. The H₂O concentration in the premixed CH₄/air flame was calculated using the total integrated absorbance area (consecutive slashes), as shown in Figure 10b. That is, as shown in absorbance equation [27], the total linestrengths in the wavelength range in which the absorption signal occurs should be included in the two partially overlapped H₂O absorption signals. Therefore, after applying the measured flame temperature to linestrength equation [24], the linestrength corresponding to the two partially overlapped H₂O absorption signals was calculated. Then, it was applied to the calculation of the H₂O concentration in the premixed CH₄/air flame by using the integrated absorbance obtained from the total partially overlapped H₂O absorption signals shown in Figure 10b. Figure 11 shows a graph comparing the flame temperature and H₂O concentration measured by TDLAS with the temperature value measured by R-type T/C and the H₂O concentration derived by Chemkin.

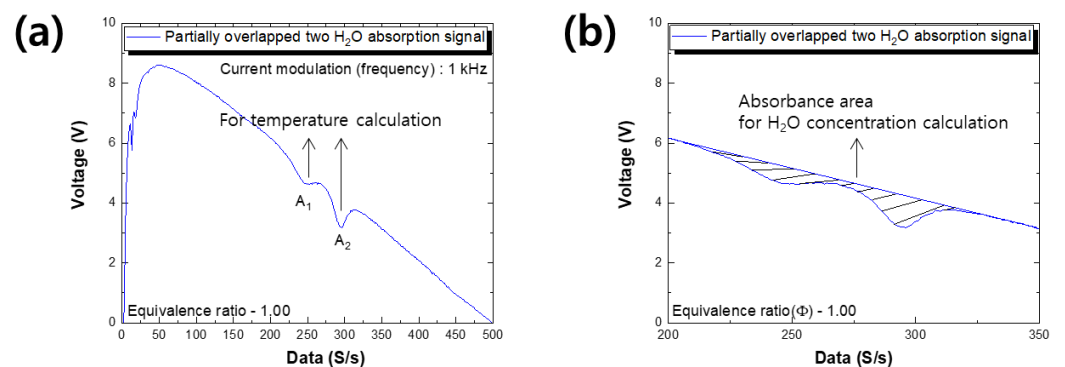


Figure 10. Two partially overlapped H₂O absorption signals (a) for measuring temperature, and (b) for measuring H₂O concentration under an equivalence ratio of 1.00.

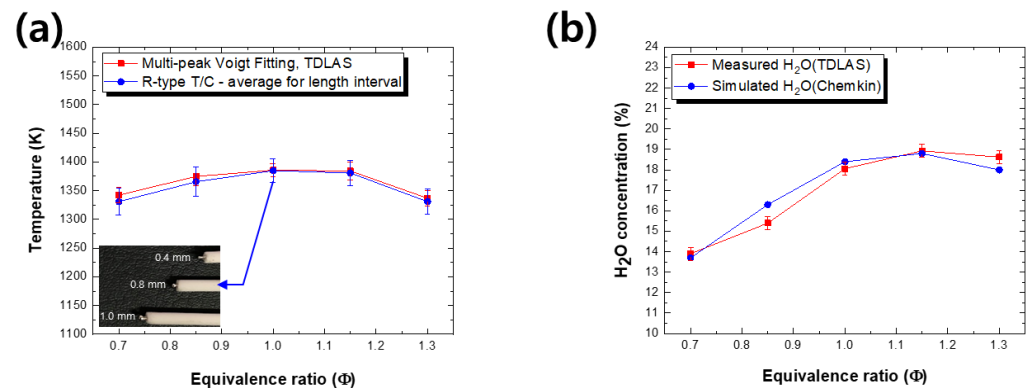


Figure 11. (a) Comparison of measured temperature using TDLAS and thermocouple, and (b) analysis of the H₂O concentration using Chemkin and TDLAS according to various equivalence ratios in a combustion environment.

Figure 11a shows the results of comparing the temperature measured using the R-type T/C and the temperature measured by the multi-peak Voigt fitting base TDLAS at a height of 5 mm above the surface of the metal fiber burner. The blue symbol in Figure 11a is the average temperature measured using R-type T/C corrected for heat loss (radiative, etc.) based on the internal length interval measurement in the flame, such as the laser path. As shown in Figure 11a, the temperature measured by the R-type T/C with various bead sizes (0.4, 0.8, and 1.0 mm) was derived by a linear function in which the temperature increased as the bead size decreased at the measured point in the flame. Then, the heat loss of R-type T/C was corrected [28]. The error bar of the blue symbol was caused by the temperature fluctuation measured by T/C in the region where the flame surface and the outside air react. That is, the temperature measured by the multi-peak Voigt fitting base TDLAS and the temperature measured by calibrated R-type T/C corrected for heat loss showed similar tendencies. In general, in the case of a premixed flame in which fuel–air is well mixed, the temperature near equivalence ratios of 1.00–1.05 has the highest value compared to when the fuel is rich or lean [29,30].

As can be seen in Figure 11a, the temperatures measured by the multi-peak Voigt fitting-based TDLAS and the temperature measured by the R-type T/C were the highest at 1385.80 and 1384.90 K, respectively at the equivalence ratio of 1.00, and the temperature decreased in the fuel-lean condition less than the equivalence ratio of 1.00. In addition, it was found that the temperature under the fuel-rich condition with an equivalence ratio of 1.00 or more decreased, as in the fuel-lean condition. When the amount of air was reduced at an equivalence ratio of 1.00 (fixed fuel rate) or more of the combustion reaction, unburned CO was generated. The temperature was expected to decrease owing to the incomplete combustion. In contrast, when the equivalence ratio was 1.00, the unreacted air cooled the heat of the flame, which lowered the flame temperature and the oxygen concentration increased [31]. Figure 11b is a graph comparing the H₂O concentration measured by TDLAS with the H₂O concentration derived by Chemkin in the premixed CH₄/air flame. Chemkin simulations were performed using a GRI 3.0 based chemical reaction mechanism suitable for CH₄/air flames, and a premixed laminar burner-stabilized flame code was considered [32]. As mentioned in the experimental setup, because the light source is transmitted to a height of 5 mm above the surface of the metal fiber burner, the simulated H₂O concentration based on a height of 5 mm above the burner surface was considered. The H₂O concentration derived from Chemkin according to the equivalence ratio decreased to 0.85 (16.30%) and 0.70 (13.70%) under the fuel lean condition. The H₂O concentration was expected to decrease significantly, owing to the increase in unreacted air in the combustion reaction under fuel-lean conditions, and the H₂O concentration under the fuel-rich condition of 1.15 (18.80%) was derived to be higher than the equivalence ratio of 1.00 (18.40%). Table 4 shows the flame temperature and concentration measured using TDLAS based on multi-peak Voigt fitting at the equivalent ratio from 0.70 to 1.30.

Table 4. Results of the temperature and concentration measured using a TDLAS-based multi-peak Voigt fitting in a premixed CH₄/air flame, and the analyzed standard deviation corresponding to the measured temperature and concentration.

Equivalence Ratio	Measured Temp. Using TDLAS (K)	Standard Deviation (\pm K)	Measured Conc. Using TDLAS (%)	Standard Deviation (\pm %)
0.70	1342.3	13.1	13.89	0.32
0.85	1374.9	16.2	15.39	0.33
1.00	1385.8	11.2	18.05	0.31
1.15	1384.3	15.6	18.92	0.32
1.30	1337.0	13.8	18.62	0.30

In addition, the measured temperature and concentration results showed standard deviation values through 10 repeated experiments. The changes in the analyzed temperature and concentration deviation were derived in the range of about 11~16 K and 0.30~0.33%, respectively. In general, the H₂O concentration was maximized when it was slightly fuel-rich ($\Phi = 1.15$), but not when it was stoichiometric. This phenomenon occurred because the heat combustion and specific heat decreased simultaneously when the equivalence ratio was larger than 1.00. That is, when the heat combustion was larger than the equivalence ratio ($\Phi = 1.05$) corresponding to the maximum temperature, it decreased more rapidly. The decrease in specific heat is a phenomenon that occurs mainly because the number of product moles decreases compared to the number of reactant moles [29,33]. Based on this result, the H₂O concentration tendency measured by TDLAS according to the various equivalence ratio is consistent with the H₂O concentration tendency calculated by Chemkin.

6. Conclusions

In this study, an experiment was conducted to measure the H₂O concentration and temperature in a premixed CH₄/air flame using two partially overlapped H₂O absorption signals based on TDLAS.

It was confirmed that the two partially overlapped H₂O absorption regions selected through the HITRAN database did not interfere with other combustion products, and the validity of the wavelengths selected from the optimal line selection method summarized by Zhou et al. was verified.

The accuracy of the temperature measurement was confirmed in the set temperature range, including the flame temperature, through a preliminary experiment using an electric furnace. To analyze the change in the sensitivity of two partially overlapped H₂O absorption signals according to the temperature, they were separated into integrated absorbance areas A1 and A2 via multi-peak Voigt fitting. The line-average temperature measured by the multi-peak Voigt fitting based TDLAS within 1073.15–1573.15 K set in the electric furnace exhibited a linear tendency when compared to the temperature measured by the T/C. Subsequently, the flame temperature and H₂O concentration were derived from the premixed CH₄/air flame based on the results of the confirmed sensitivity in the preliminary experiment. The temperature measured by the multi-peak Voigt fitting based on the TDLAS and the temperature measured by the T/C corrected for heat loss under lean fuel conditions showed the same tendency, and the highest temperature was measured at an equivalence ratio of 1.00. In the case of the H₂O concentration in the premixed CH₄/air flame, the H₂O concentration derived using the GRI 3.0 mechanism of Chemkin was compared with the H₂O concentration measured by TDLAS. The H₂O concentration derived from the Chemkin simulation decreased sharply under fuel-lean conditions, and the highest H₂O concentration was derived in the fuel-rich region 1.15. Hence, it was consistent with the tendency of H₂O concentration measured by TDLAS. This study focused on whether it is possible to accurately measure the temperature and H₂O concentration using two partially overlapped H₂O absorption signals. In conclusion,

the two partially overlapped H₂O absorption signals can provide good results and are expected to be effective in measuring the internal temperature and H₂O concentration of large combustion systems.

Author Contributions: Conceptualization, S.S.; methodology, S.S.; software, S.S.; validation, J.H., D.K. and C.L.; formal analysis, S.S.; investigation, S.S., N.J.; resources, C.L.; data curation, S.S.; writing—original draft preparation, S.S.; writing—review and editing, C.L.; visualization, S.S., N.J. and A.S.; supervision, C.L.; project administration, C.L.; funding acquisition, C.L. All authors have read and agreed to the published version of the manuscript.

Funding: This work was supported by the KIST Institutional Program (Project No. 2E31340-21-P012).

Institutional Review Board Statement: Not applicable.

Informed Consent Statement: Not applicable.

Data Availability Statement: The data presented in this study are available on request from the corresponding author.

Conflicts of Interest: The authors declare no conflict of interest. The funders had no role in the design of the study; in the collection, analyses, or interpretation of data; in the writing of the manuscript, or in the decision to publish the results.

Nomenclature

ΔE_i	Uncertainty of energy level
τ	Lifetime
α_v	Absorbance of multiple transitions
ϕ_V	Voigt function
ν	Wavelength
$\nu_{0,i}$	Peak position
γ_i	Half-width at half maximum
M	The number of peaks
i	The serial number of each peak
γ_D	Doppler's half-width at half maximum
γ_L	Lorentzian's half-width at half maximum
M_{mole}	Molecular weight
E	Lower-state energy
R	Linestrength ratio

References

- U.S. Energy Information Administration. *Annual Energy Outlook*; U.S. Energy Information Administration: Washington, DC, USA, 2020.
- Qu, Z.; Steinvall, E.; Ghorbani, R.; Schmidt, F.M. Tunable diode laser atomic absorption spectroscopy for detection of potassium under optically thick conditions. *Anal. Chem.* **2016**, *88*, 3754–3760. [[CrossRef](#)]
- Witzel, O.; Klein, A.; Meffert, C.; Schulz, C.; Kaiser, S.; Ebert, V. Calibration-free, high-speed, in-cylinder laser absorption sensor for cycle-resolved, absolute H₂O measurements in a production IC engine. *Proc. Combust. Inst.* **2015**, *35*, 3653–3661. [[CrossRef](#)]
- Sepman, A.; Ögren, Y.; Qu, Z.; Wiinikka, H.; Schmidt, F.M. Real-time in situ multi-parameter TDLAS sensing in the reactor core of an entrained-flow biomass gasifier. *Proc. Combust. Inst.* **2017**, *36*, 4541–4548. [[CrossRef](#)]
- Spearrin, R.M.; Goldenstein, C.S.; Schultz, I.A.; Jeffries, J.B.; Hanson, R.K. Simultaneous sensing of temperature, CO, and CO₂ in a scramjet combustor using quantum cascade laser absorption spectroscopy. *Appl. Phys. A* **2014**, *117*, 689–698. [[CrossRef](#)]
- Sur, R.; Sun, K.; Jeffries, J.B.; Socha, J.G.; Hanson, R.K. Scanned-wavelength-modulation-spectroscopy sensor for CO, CO₂, CH₄ and H₂O in a high-pressure engineering-scale transport-reactor coal gasifier. *Fuel* **2015**, *150*, 102–111. [[CrossRef](#)]
- Witzel, O.; Klein, A.; Meffert, C.; Wagner, S.; Kaiser, S.; Schulz, C.; Ebert, V. VCSEL-based, high-speed, in situ TDLAS for in-cylinder water vapor measurements in IC engines. *Opt. Express* **2013**, *21*, 19951–19965. [[CrossRef](#)] [[PubMed](#)]
- Hanson, R.K.; Falcone, P.K. Temperature measurement technique for high-temperature gases using a tunable diode laser. *Appl. Opt.* **1978**, *17*, 2477–2480. [[CrossRef](#)] [[PubMed](#)]
- Webber, M.E.; Wang, J.; Sanders, S.T.; Baer, D.S.; Hanson, R.K. In situ combustion measurements of CO, CO₂, H₂O and temperature using diode laser absorption sensors. *Proc. Combust. Inst.* **2000**, *28*, 407–413. [[CrossRef](#)]
- Torek, P.V.; Hall, D.L.; Miller, T.A.; Wooldridge, M.S. H₂O absorption spectroscopy for determination of temperature and H₂O mole fraction in high-temperature particle synthesis systems. *Appl. Opt.* **2002**, *41*, 2274–2284. [[CrossRef](#)] [[PubMed](#)]

11. Goldenstein, C.S.; Jeffries, J.B.; Hanson, R.K. Diode laser measurements of linestrength and temperature-dependent lineshape parameters of H₂O-, CO₂-, and N₂-perturbed H₂O transitions near 2474 and 2482nm. *J. Quant. Spectrosc. Radiat. Transf.* **2013**, *130*, 100–111. [CrossRef]
12. Wu, K.; Li, F.; Cheng, X.; Yang, Y.; Lin, X.; Xia, Y. Sensitive detection of CO₂ concentration and temperature for hot gases using quantum-cascade laser absorption spectroscopy near 4.2 μm. *Appl. Phys. A* **2014**, *117*, 659–666. [CrossRef]
13. Ma, L.H.; Lau, L.Y.; Ren, W. Non-uniform temperature and species concentration measurements in a laminar flame using multi-band infrared absorption spectroscopy. *Appl. Phys. A* **2017**, *123*, 83. [CrossRef]
14. Wei, W.; Peng, W.Y.; Wang, Y.; Shao, J.; Strand, C.L.; Hanson, R.K. Two-color frequency-multiplexed IMS technique for gas thermometry at elevated pressures. *Appl. Phys. A* **2020**, *126*, 1–16. [CrossRef]
15. Bao, Y.; Zhang, R.; Enemali, G.; Cao, Z.; Zhou, B.; McCann, H.; Liu, C. Relative entropy regularized TDLAS tomography for robust temperature imaging. *IEEE Trans. Instrum. Meas.* **2021**, *70*, 1–9. [CrossRef]
16. Zhou, X.; Liu, X.; Jeffries, J.B.; Hanson, R.K. Development of a sensor for temperature and water concentration in combustion gases using a single tunable diode laser. *Meas. Sci. Technol.* **2003**, *14*, 1459–1468. [CrossRef]
17. Wang, Z.; Fu, P.; Chao, X. Laser absorption sensing systems: Challenges, modeling, and design optimization. *Appl. Sci.* **2019**, *9*, 2723. [CrossRef]
18. Penner, S.S. *Quantitative Molecular Spectroscopy and Gas Emissivities*, 1st ed.; Addison-Wesley: Boston, MA, USA, 1959.
19. Hanson, R.K.; Spearrin, R.M.; Goldenstein, C.S. *Spectroscopy and Optical Diagnostics for Gases*; Springer: Cham, Switzerland, 2016.
20. Zhou, S.; Yang, W.; Liu, C.; Zhang, L.; Yu, B.; Li, J. CO₂-broadening coefficients for the NO₂ transitions at 6.2 μm measured by mid-infrared absorption spectroscopy. *J. Quant. Spectrosc. Radiat. Transf.* **2020**, *242*, 106754. [CrossRef]
21. Yang, W.; Li, B.; Zhou, J.; Han, Y.; Wang, Q. Continuous-wavelet-transform-based automatic curve fitting method for laser-induced breakdown spectroscopy. *Appl. Opt.* **2018**, *57*, 7526–7532. [CrossRef] [PubMed]
22. Gordon, I.E.; Rothman, L.S.; Hill, C.; Kochanov, R.V.; Tan, Y.; Bernath, P.F.; Birk, M.; Boudon, V.; Campargue, A.; Chance, K.V.; et al. The HITRAN 2016 molecular spectroscopic database. *J. Quant. Spec. Radiat. Transf.* **2017**, *203*, 3–69. [CrossRef]
23. So, S.; Park, J.; Song, A.; Hwang, J.; Yoo, M.; Lee, C. Detection limit of CO concentration measurement in LPG/air flame flue gas using tunable diode laser absorption spectroscopy. *Energies* **2020**, *13*, 4234. [CrossRef]
24. Goldenstein, C.S.; Spearrin, R.M.; Jeffries, J.B.; Hanson, R.K. Infrared laser-absorption sensing for combustion gases. *Prog. Energy Combust. Sci.* **2017**, *60*, 132–176. [CrossRef]
25. Zhou, X. Diode-Laser Absorption Sensors for Combustion Control. Ph.D. Thesis, Stanford University, Stanford, CA, USA, 2005.
26. Bolshov, M.; Kuritsyn, Y.; Romanovskii, Y. Tunable diode laser spectroscopy as a technique for combustion diagnostics. *Spectrochim. Acta Part B At. Spectrosc.* **2015**, *106*, 45–66. [CrossRef]
27. Liu, C.; Xu, L. Laser absorption spectroscopy for combustion diagnosis in reactive flows: A review. *Appl. Spectrosc. Rev.* **2019**, *54*, 1–44. [CrossRef]
28. Hindasageri, V.; Vedula, R.P.; Prabhu, S.V. Thermocouple error correction for measuring the flame temperature with determination of emissivity and heat transfer coefficient. *Rev. Sci. Instrum.* **2013**, *84*, 024902. [CrossRef] [PubMed]
29. Stephen, R.T. *An Introduction to Combustion: Concepts and Applications*, 2nd ed.; McGraw-Hill Education: New York, NY, USA, 2002.
30. Lee, J.; Bong, C.; Yoo, J.; Bak, M.S. Combined use of TDLAS and LIBS for reconstruction of temperature and concentration fields. *Opt. Express* **2020**, *28*, 21121–21133. [CrossRef]
31. So, S.; Park, D.G.; Jeong, N.; Kim, D.; Hwang, J.; Lee, C. Study on the simultaneous measurement of O₂ and CO concentrations in the exhaust gas of a methane/air flame using tunable diode laser absorption spectroscopy. *Energy Fuels* **2020**, *34*, 3780–3787. [CrossRef]
32. Smith, G.P.; Golden, D.M.; Frenklach, M.; Moriarty, N.W.; Eiteneer, B.; Goldenberg, M.; Bowman, C.T.; Hanson, R.K.; Song, S.; Gardiner, W.C.; et al. GRI-Mech 3.0. Available online: http://www.meberkeley.edu/gri_mech/ (accessed on 15 February 2021).
33. Law, C.K. *Combustion Physics*, 1st ed.; Cambridge University Press: New York, NY, USA, 2006.